400 MPa 级超级钢专用焊条

赵洪运，　徐春华，　杨贤群，　吴剑谦
（哈尔滨工业大学（威海）材料科学与工程学院，山东 威海　264209）

摘　要：焊缝金属的强韧化是超级钢焊接中的一个技术难题，要实现焊缝的强韧化，并避免冷裂纹，需开发与母材性能相匹配的焊接材料。对 400 MPa 级超级钢主要通过合金化控制焊缝组织使其获得针状铁素体即可获得理想的强韧性。通过大量工艺试验研究，结合 400 MPa 级超级钢的组织性能特点，研制开发了一种 400 MPa 级超级钢专用焊条。检测结果表明，该种焊条形成的焊缝金属组织为细小针状铁素体，焊缝金属屈服强度为 435 MPa，抗拉强度为 612 MPa，冲击吸收功为 148 J，其组织和性能同 400 MPa 级超级钢能很好的相匹配，达到了预期目的。

关键词：400 MPa 级超级钢；合金化；针状铁素体
中图分类号：TG115.28　　文献标识码：A　　文章编号：0253－360X(2007)10－013－04

赵洪运

0　序　　言

焊缝金属的强韧化是超级钢焊接中的一个技术难题，并且随着强度级别的提高，碳当量增大，焊缝的冷裂倾向增大。要实现焊缝的强韧化，并避免冷裂纹，需开发与母材性能相匹配的焊接材料。

焊接材料主要是通过合金化控制焊缝的组织实现强韧化，对 400 MPa 级超级钢主要通过调整焊缝组织使其获得针状铁素体来获得理想的强韧性。

文中通过大量工艺试验研究，结合 400 MPa 级超级钢的组织性能特点，研制开发一种与其组织性能相匹配的专用焊接材料，同时也为更高强度级别的超级钢专用焊接材料的研制开发提供理论依据和经验。

1　试　　验

1.1　试验材料

选用 H08A 作为焊条的焊芯（ϕ3.2 mm），其化学成分见表 1。焊接工艺试验是在 400 MPa 级超级钢板上进行的，晶粒尺寸为 5～7 μm，规格为 130 mm×80 mm×5 mm。其化学成分见表 2，主要力学性能指标见表 3。

表 1　焊条焊芯的化学成分（质量分数，%）

Table 1　Chemical composition of welding center

C	Mn	Si	Cr	S	P	Ni
0.10	0.3～0.55	0.03	0.20	0.03	0.03	0.30

表 2　400 MPa 级超级钢的化学成分（质量分数，%）

Table 2　Chemical composition of 400 MPa ultra-fine grained steel

C	Mn	Si	P	S	Al	Cu	Cr	Mo	Ni
0.12	0.36	0.09	0.013	0.013	0.025	0.01	0.02	0.01	0.03

表 3　400 MPa 级超级钢的力学性能

Table 3　Mechanical properties of 400 MPa ultra-fine grained steel

下屈服强度 R_{eL}/MPa	抗拉强度 R_m/MPa	断后伸长率 A(%)	硬度 HV	冲击吸收功 $A_{kv0\ ℃}$/J
405	578	21	158	108.6

药皮原料为人造金红石、还原钛铁矿、长石、云母、白泥、中碳锰铁、钛白粉、大理石、金属铬、钼铁、钛铁、硼、稀土、水玻璃等。

1.2　试验方法

采用 ZXG1－400 型直流弧焊焊机，并用设计好的焊条在母材（400 MPa 级超级钢）上施焊，焊后要把熔渣清理干净，避免产生夹杂，焊接工艺参数见表 4。

收稿日期：2007－06－08
基金项目：国家“863”高技术研究发展计划资助项目（2001AA332020）

表 4 焊接工艺参数

Table 4 Welding parameter

焊接极性	焊接电流 I/A	焊接速度 v/(mm·min^{-1})	焊后状态
直流反接	110	80	空冷

用 JSM—5500LV 扫描电镜和 MM—6 型金相显微镜对焊接接头焊缝金属进行显微组织观察、分析，腐蚀液采用 4%HNO_3 酒精溶液。

用 HXD—1000 型显微硬度计测定焊缝金属组织显微硬度，载荷 100 g，加载时间 15 s。

将焊条电弧焊焊接试样，制成拉伸试样后，放在液压万能试验机上进行拉伸试验。计算出每个试样的抗拉强度和屈服强度。

2 400 MPa 超级钢专用焊条配方设计

2.1 焊条配方的初步设计

焊条药皮选用钛钙型药皮；经多次试验优选，取焊条药皮重量系数 K=0.4，试验所用 H08A 焊芯取直径 d=3.2 mm，长度 L=350 mm，得焊条药皮质量 m=5.0 g，焊条药皮外径 D=5.0～5.2 mm，满足条件 $D/d \leqslant 2.1$。

相关文献[1]给出了需要向焊条配方中添加的一定量合金元素的作用，包括 Cr，Mo，Ti，B 和稀土元素。药皮矿物原料选用人造金红石、还原钛铁矿、长石、云母、白泥、中碳锰铁、钛白粉、大理石、水玻璃。采用正交试验法对药皮矿物原料选用量进行比较分析，确定的药皮矿物原料含量见表 5。通过计算得出熔渣碱度 B=0.631 7，熔渣呈弱酸性，比较利于合金元素的过渡，达到了预期设计要求[2]。

表 5 药皮矿物原料含量(质量分数，%)

Table 5 Contents of medical berry mineral material

成 分	含 量
人造金红石	24.0
还原钛铁	6.0
大理石	19.0
钛白粉	7.0
中碳锰铁	12.0
白泥	14.0
长石	8.0
云母	5.0
水玻璃	适量

2.2 合金元素含量的确定

焊条药皮中矿物原料含量确定后(表 5)，在试验过程中对合金元素含量进行了调整，见表 6，并根据最后检验结果最终确定出最佳焊条配方。

表 6 焊条药皮配方(质量分数，%)

Table 6 Formulation of electrode covering

	Mo	Cr	Ti	B	Ce
NO. 1	6	2	—	—	—
NO. 2	2	6	—	—	—
NO. 3	4	2	1	0.15	0.85

3 专用焊接材料焊缝组织性能分析

3.1 焊缝金属组织观察与分析

选用 J422 焊条(ϕ3.2 mm)和试验制备成的超级钢专用焊条(ϕ3.2 mm)，分别按表 4 进行焊接试验。然后截取焊接接头，经磨光、抛光，用 4%HNO_3 酒精溶液腐蚀后，制成金相试样，并进行对比分析。所得的焊缝金相组织形貌如图 1，图 2，图 3 和图 4 所示。

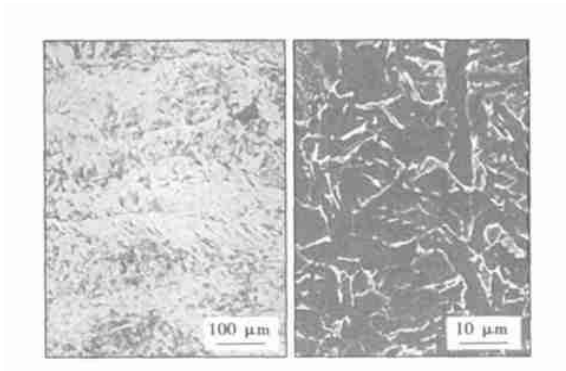

图 1 J422 焊缝组织光镜和扫描电镜形貌

Fig. 1 SEM microstructure of weld of J422 electrode

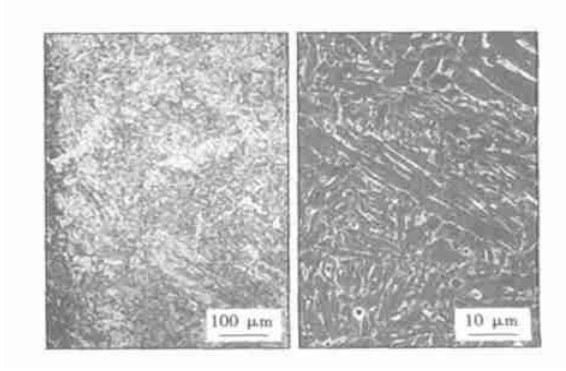

图 2 NO. 1 焊缝组织光镜和扫描电镜形貌

Fig. 2 SEM microstructure of No1 weld

从图1可以看到粗大的柱状晶，粗大的块状先

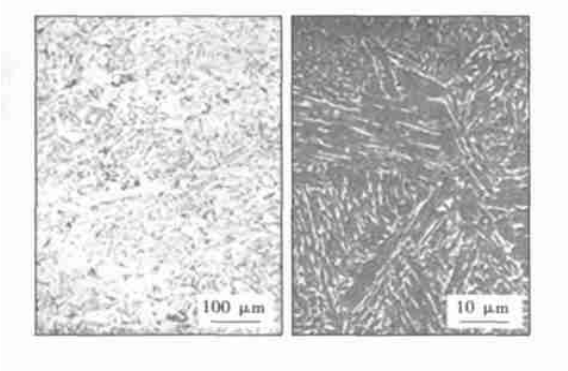

图 3　NO. 2 焊缝组织光镜和扫描电镜形貌

Fig 3　SEM microstructure of No2 weld

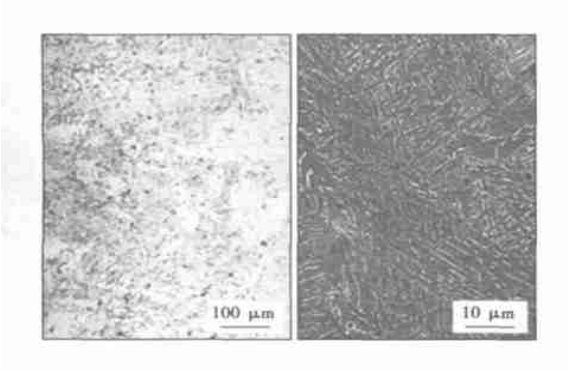

图 4　NO. 3 焊缝组织光镜和扫描电镜形貌

Fig 4　SEM microstructure of No3 weld

共析铁素体和珠光体组织。焊缝柱状晶首先在母材的部分熔化区晶粒表面连生长大，晶体长大方向垂直于熔池金属与母材金属的分界面，沿结晶方向长大。焊缝先共析铁素体是焊缝在凝固结晶全部生成柱状晶的奥氏体以后，固相的铸态奥氏体组织首先发生相变析出的组织。晶界先共析铁素体析出后，会由于碳的扩散提高晶界附近碳浓度靠近晶界先共析铁素体处形成珠光体组织。

从图 2 可以看到，随着焊缝中含钼量的增加，原始奥氏体晶界的铁素体逐渐减少，最后几乎完全消失。针状铁素体的板条尺寸减小，而马氏体/奥氏体二次相体积分数增加。最后，针状铁素体被含有二次相的铁素体所取代。焊缝组织由于添加钼而发生了细化。

从图 3 可以看出焊缝组织有所细化，没有粗大的柱状晶组织，先共析铁素体的量有所减少，粗晶区特征消失，出现了少量的针状铁素体。针状铁素体属于贝氏体范畴的组织，生长在晶粒内部，具有很好的韧性。焊缝组织由于添加了铬而显得十分均匀。此外，在原奥氏体晶界发现有碳化物析出。

从图 4 可以看出组织明显细化，先共析铁素体的量减少，针状铁素体的量增多，出现了少量的等轴晶。这是由于又添加了一定量的 Mo，Ti，B，稀土合金元素，这些合金元素形成了碳化物，作为核心形成更多的晶核，促使柱状晶细化，使焊缝的等轴晶区加宽，焊缝组织得到细化。

3.2　焊缝金属显微硬度测试结果与分析

利用显微硬度计分别对 J422，NO. 1，NO. 2 和 NO. 3 焊条焊接接头进行硬度检测，结果如图 5 所示。由图 5 可以看出，J422 焊条的焊缝金属组织的显微硬度值较其它三种焊条都低，这是由于 J422 焊条配方中没有添加一定量的合金元素，焊缝组织中没有形成高硬度碳化物。而 NO. 1，NO. 2，NO. 3 三种焊条的焊缝金属组织的显微硬度值要比 J422 高很多，且 NO. 3 焊条要比 NO. 1 和 NO. 2 焊条稍高些。这是因为 NO. 1 焊条配方中主要添加了一定量的 Mo；NO. 2 焊条配方中主要添加了一定量的 Cr；NO. 3 焊条配方中除了添加 Mo，Cr 元素外，又多添加了少量的 Ti，B 和稀土合金元素，其中 Cr 是易固溶于铁素体的合金元素，可使铁素体的硬度和强度增高。Mo，Ti，B 是在铁素体中有限固溶的元素，在焊缝结晶和冷却过程中易析出碳化物，也可以提高焊缝金属的强度和硬度，此外 Cr，Mo，Ti，B 及稀土元素还可以细化晶粒，通过细化晶粒的强化方式来提高焊缝强度和硬度。

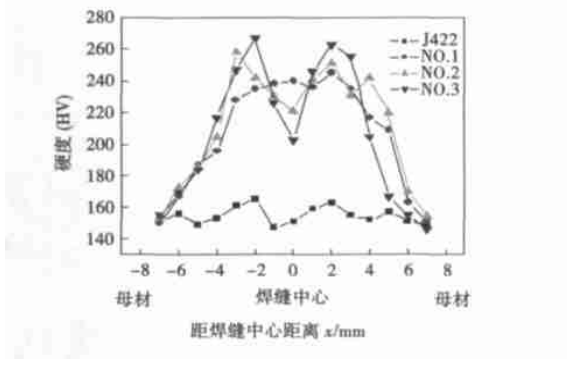

图 5　焊接接头硬度分布曲线

Fig 5　Distribution of hardness of welded joint

3.3　焊缝金属力学性能分析

为检验 J422，NO. 1，NO. 2 和 NO. 3 焊条焊缝金属的力学性能，分别对这几种焊接材料所得焊缝金属进行拉伸和冲击试验，强度检测结果见表 7，冲击检测结果见表 8。

由强度检测结果和冲击试验结果可以看出，

表 7 强度检测结果

Table 7 Test result of strength test

	下屈服强度 R_{eL}/ MPa	抗拉强度 R_m/ MPa		下屈服强度 R_{eL}/MPa	抗拉强度 R_m/MPa
J 422	348	428	NO. 2	402	435
NO. 1	413	586	NO. 3	580	612

表 8 冲击试验结果

Table 8 Test result of impact test

	冲击吸收功 $A_{KV(20\ ℃)}$/ J		冲击吸收功 $A_{KV(20\ ℃)}$/ J
J 422	67	NO. 2	117
NO. 1	131	NO. 3	148

J422 焊条的焊缝金属不论是强度还是冲击吸收功都最低, 且低于母材的相应指标; NO. 1, NO. 2 焊条的强度与母材相当, 且冲击功高于母材; NO. 3 焊条不论是强度还是冲击功都最高, 且明显高于母材。

3.4 综合分析

由上述试验结果不难看出, 从焊逢金属组织形态、晶粒尺寸和性能指标来看, NO. 3 配方为最佳配方。

4 结 论

(1) 试验过程中采用正交试验方法, 既减少了试验的工作量和成本, 又得到了满意的效果。

(2) 专用焊条选用 H08A 为焊芯, 通过在焊条药皮中加入少量合金元素改善焊缝组织和性能, 不仅成本低廉, 而且焊接工艺性能优良。

(3) 用专用焊条焊接 400 MPa 级超级钢, 各项性能指标均高于母材。

参考文献:

[1] 尹士科. 焊条材料实用基础知识[M]. 北京: 化学工业出版社, 2004.

[2] 韩永传. 熔渣碱度对焊条药皮中合金元素过渡系数的影响[J]. 水利电力机械, 1999(1): 23-25.

作者简介: 赵洪运, 男, 1966 年出生, 博士, 教授。主要从事焊接材料与工艺方面的科研和教学工作。发表论文 40 余篇。

Email: hy_zhao66@163.com

MAIN TOPICS, ABSTRACTS & KEY WORDS

Simulation and experimental investigations of laser cladding temperature field on 6061 Al alloy ZHANG Song[1], ZHANG Chunhua[1,2], ZHANG Ning[1], YU Lili[1], LIU Changsheng[2], Man H C[3] (1. School of Material Science & Engineering, Shenyang University of Technology, Shenyang 110023, China; 2. School of Material & Metallurgy, Northeastern University, Shenyang 110004, China; 3. Department of Industrial & Systems Engineering, The Hongkong Polytechnic University, Hongkong, China). p1—4

Abstract: According to the characters of laser cladding, a computational model was established for analysis of 3D laser cladding temperature field caused by moving gauss distribution heat source and laser cladding temperature field of 6061 Al alloy was simulated dynamically by finite element method with software ANSYS. The results show that the isotherms of temperature field simulation look like ellipse and are dense at the head of the moving heat source. And the temperature gradient is high at the head of the moving heat source. But at the end of the moving heat source the isotherms are sparse and the temperature gradient is low. With continuous wave Nd: YAG laser, SiC ceramic powder was cladded on the 6061 Al alloy surface and the SiC reinforced metal matrix composites (MMC) modified layer was abtained. Al, SiC and Al_4C_3, and a little Al_4SiC_4 were included in this layer. It was shown that the simulation results of temperature field are in accordance with the experimental results. It offers the reliance for the optimization of the laser parameters on metal matrix composites.

Key words: laser cladding; metal matrix composite; temperature field; finite element method

Through-thickness diversity of properties in friction stir welded 2219—T87 thick aluminum alloy plate ZHOU Pengzhan[1,2], LI Donghui[1], HE Diqiu[1], DENG Hang[1] (1. School of Mechanical and Electrical Engineering, Central South University, Changsha 410083, China; 2. Zhuzhou Times New Materials Technology Co. Ltd., Zhuzhou 412007, Hunan, China). p5—8

Abstract: Friction stir welding of 2219—T87 high-strength aluminum alloy plate in 35 mm thickness was completed with a single pass. The results demonstrate that the tensile strength of weld reaches 274 MPa, and the fracture happens in the WNZ (welding nugget zone). Because the welding speed was slow for welding thick plate, and the temperature of the upper WNZ was higher, the microstructure became coarse under the pumping action of screwed stirrer. While the temperature of the bottom WNZ was lower, the microstructure became compact under the crushing action of screwed stirrer. The microhardness of upper WNZ had a decrease zone, while that of bottom changed slowly. When the welding thickness was too large, the microstructure of upper WNZ will become coarse for pumping of screwed stirrer, and it can cause microhardness decrease. It was the reason why the tensile property not high and the fracture was located in the WNZ.

Key words: friction stir welding of thick plate; 2219—T87 aluminum alloy; through-thickness

Diffusion bonding of Mg/Al alloy with Zn interlayer metal ZHAO Limin, LIU Liming, XU Rongzheng, ZHANG Zhaodong (State Key Laboratory of Materials Modification by Laser, Ion and Electron Beams, Dalian University of Technology, Dalian 116024, Liaoning, China). p9—12

Abstract: The characteristics of microstructure and mechanical properties of the Mg/Al alloy joint by diffusion bonding with a Zn interlayer were studied by means of metalloscopy, X-ray diffraction, electron probe microanalysis and mechanical property test. Investigations showed that the Mg/Al alloy joint by diffusion bonding with Zn interlayer consists of a multilayer sandwich structure, including the transition zone of Zn-Al, the residual Zn interlayer, as well as the transition zone of Zn-Mg. The transition zone of Zn-Al is composed mainly of a solid solution structure, while the Zn-Mg transition zone has a relative larger dimension after a rapid eutectic reaction. The addition of zinc interlayer inhibits the inter-diffusion of Mg and Al alloy efficiently. The Zn-Mg transition zone constitutes the main part of the joint and consists of Mg and the new phases formed are Mg_2Zn_{11} and $MgZn_2$ intermetallic compound. According to the phase constitution analyses executed on each side of the fracture face, it was deduced that the fracture of Mg/Al alloy joint located around the interface of Zn-Mg transition zone. The average shear strength of Mg/Al alloy joints diffusion bonded with Zn interlayer reaches 70 MPa and exceeds that of the joints bonded without Zn interlayer enormously.

Key words: magnesium alloy; aluminum alloy; zinc interlayer; diffusion bonding; joint strength

Special-purpose electrode for 400 MPa grade ultrafine grained steel ZHAO Hongyun, XU Chunhua, YANG Xianqun, WU Jianqian (School of Materials Science and Engineering, Harbin Institute of Technology at Weihai, Weihai 264209, Shandong, China). p13—16

Abstract: The strengthening and toughening of weld metal is a technical difficulty of ultrafine grained steel welding, and it needs to develop a kind of welding material matching the base metal in order to realize the strengthening and toughening of welded joint and avoid the cold crack. The ideal strength and toughness can be obtained by alloying mathod and controling weld structure to obtain the acicular ferrites. Through experiments, and unifying the microstructure and mechanical properties characteristics of 400 MPa grade ultrafine grained steel, a special-purpose electrode of 400 MPa grade ultrafine grained steel was develeped. The examination results show that, the microstructures of weld metal by this electrode are tiny acicular ferrites, and the yield strength and teusile strength of the welded joint are 435 MPa and 612 MPa, respectively. The impact absorbing energy is 148 J. Its microstructures and mechanical properties match the 400 MPa grade ultrafine grained steel well, and achieve the anticipated goal.

Key words: 400 MPa grade ultrafine gaind steel; alloying; acicular ferrite

Mechanical properties and microstructure features of linear friction welded TC4 titanium alloy joint MA Tiejun, YANG Siqian, ZHANG Yong, LI Wenya (College of Material Science and Engineering, Northwestern Polytechnical University, Xi'an 710072, China). p17—20

Abstract: The linear friction welding (LFW) experiment of TC4 titanium alloy was carried out with homemade LFW machine (XMH—160). Joints with 100% joining rate were obtained under the optimum parameters based on the experiments. All the tensile test specimens fractured in the base metal of TC4 at a place far form the weld, which indicated that the mechanical properties of the weld are higher than those of the base metal. The microstructure of the joint was observed, and it showed that the thickness of the weld is about 60 μm at the central zone and around 110 μm at the marginal zone, and the metal streamline are distributed symmetrically on both sides of weld. The weld consists of the superfine α + β strucure, and the zone close to the weld consists of α and β phases deformed in different degree, but they did not grow up obviously. The microhardness of the weld is higher than that of the base metal markedly. It is the microstructure features of the weld that contribute to the higher tensile properties and microhardness than those of the base metal.

Key words: TC4 titanium alloy; linear friction welding; mechanical properties; microstructure; microhardness

Effects of activating fluxes on DCSP A-TIG weld penetration of magnesium alloy HUANG Yong, FAN Ding, LIN Tao, SHAO Feng (State Key Laboratory of Gansu Advanced Non-ferrous Metal Materials, Lanzhou University of Technology, Lanzhou 730050, China). p21—24

Abstract: DCSP (direct current straight polarity) A-TIG (activating-tungsten inert gas) welding experiments of magnesium alloy were carried out to study the effects of surface activating fluxes on weld penetration. Elements including Te, Ti and Si, and oxides including SiO_2, TiO_2 and V_2O_5, and halides including $MnCl_2$, $CdCl_2$ and ZnF_2 were used as activating fluxes, respectively. It is found, the weld penetration and width of Te powder reach 2.5 times and 1.4 times of those of conventional TIG welding, respectively. Ti and Si have small effects. Both V_2O_5 and SiO_2 increase weld penetration and width. Especially for SiO_2, the weld penetration and width reach 2.0 and 1.6 times of those of conventional TIG welding. TiO_2 has small effect. All ZnF_2, $CdCl_2$ and $MnCl_2$ increase weld penetration and width obviously. The effect of ZnF_2 is the most dramatic. The weld penetration and width reach 4.0 and 1.6 times of those of conventional TIG welding. It is believed that, the mechanism of activating fluxes improving weld penetration of DCSP A-TIG welding of magnesium alloy is relative to heat input increase because of activating fluxes constricting arc.

Key words: magnesium alloy; direct current straight polarity activating-tungsten inert gas welding; activating flux; weld penetration

Influence of transitive materials on Al_2O_3 gradient ceramic coatings prepared by plasma spraying LEI Ali, LI Gaohong, FENG Lajun, XU Dapeng (School of Materials Science and Engineering, Xi'an University of Technology, Xi'an 710048, China). p25—28

Abstract: According to the fact that Al_2O_3 ceramic coatings have low adhesion strength and high porosity, two kinds of Al_2O_3 gradient ceramic coatings using NiAl intermetallic compound and Cu powders as transitive materials respectively were prepared by plasma spraying, and the microstructure of gradient coatings was observed, and the adhesion strength and porosity of the coatings were tested and analyzed. The results indicate that the gradient coatings show that the characteristic of structure is not uniform macroscopically but consecutive microscopically. NiAl intermetallic compound and Cu are ideal transitive materials between metal matrix and Al_2O_3 coatings, which can improve the adhesion strength of the coatings efficiently. The adhesion strength of Cu-Al_2O_3 gradient coatings is higher than that of NiAl-Al_2O_3 gradient coatings. The porosity of gradient coatings is lower than that of double layer coatings. The porosity of Cu-Al_2O_3 gradient coatings decreases as the Al_2O_3 content increases, and it is lower than that of NiAl-Al_2O_3 gradient coatings.

Key words: plasma spraying; gradient coatings; Al_2O_3 ceramic coatings

Influences of firing parameters on properties and microstructure of Ni-Cr alloy and porcelain interface LIU Jie[1], QIU Xiaoming[1], ZHU Song[2], SUN Daqian[1] (1. College of Materials Science and Engineering, Jilin University, Changchun 130022, China; 2. Tomatological Hospital, Jilin University, Changchun 130041, China). p29—32

Abstract: The influence of altering firing temperature and time on the mechanical properties and microstructure of the meatal-porcelain interface were studied. The experimental results showed that the reaction in the metal-porcelain interface was very complicated, and the phases of metal-porcelain interface were mainly SnO_2, $SnCr_{0.14}O_x$, $AlNi_3$, $KAlSi_2O_6$ composite oxides etc. The kinds, quantities and distributions of the interface reaction products were affected by vaviations of firing technological parameters changing, which finally determined bonding strength of metal-porcelain interface. In certain range, the interfical reaction layers widened and the mutant metal-porcelain interface changed into compound type as firing temperature increaseing and firing time prolonging, which played an important role in increasing metal-porcelain interface bonding strength. The bonding strength was 42.7 MPa with firing temperature of 960 ℃ and firing time of 2.5 min.

Key words: Ni-Cr alloy; metal-porcelain interface; mechanical properties; microstructure

Reactive synthesis TiN reinforced matrix composite coating by electric-spark deposition HAO Jianjun[1,2], HUANG Jihua[1], ZHAO Jianguo[2], CHEN Zhiqiang[2] (1. School of Materials Science and Engineering, University of Science and Technology of Beijing, Beijing 100083, China; 2. College of Electromechanical Engineering, Agriculture University of Hebei, Baoding 071001, Hebei, China). p33—36

Abstract: TiN metal matrix composite coating was deposited